SUPPLEMENTARY INFORMATION FOR
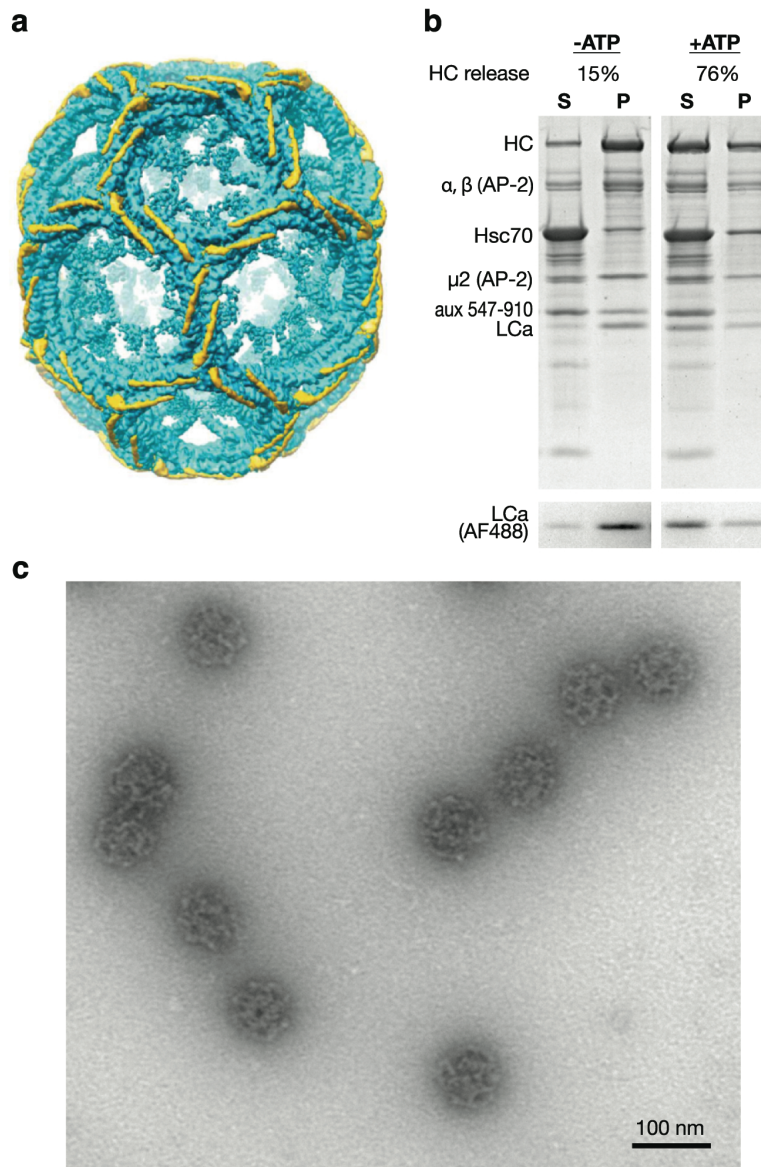
Single-molecule analysis of a molecular disassemblase reveals the mechanism of Hsc70-driven clathrin uncoating

Till Böcking[1,2], François Aguet[2], Stephen C. Harrison[3], Tomas Kirchhausen*[1,2]

[1]Immune Disease Institute, [2]Department of Cell Biology, [3]Department of Biological Chemistry and Molecular Pharmacology and Howard Hughes Medical Institute, Harvard Medical School, Boston, MA 02115
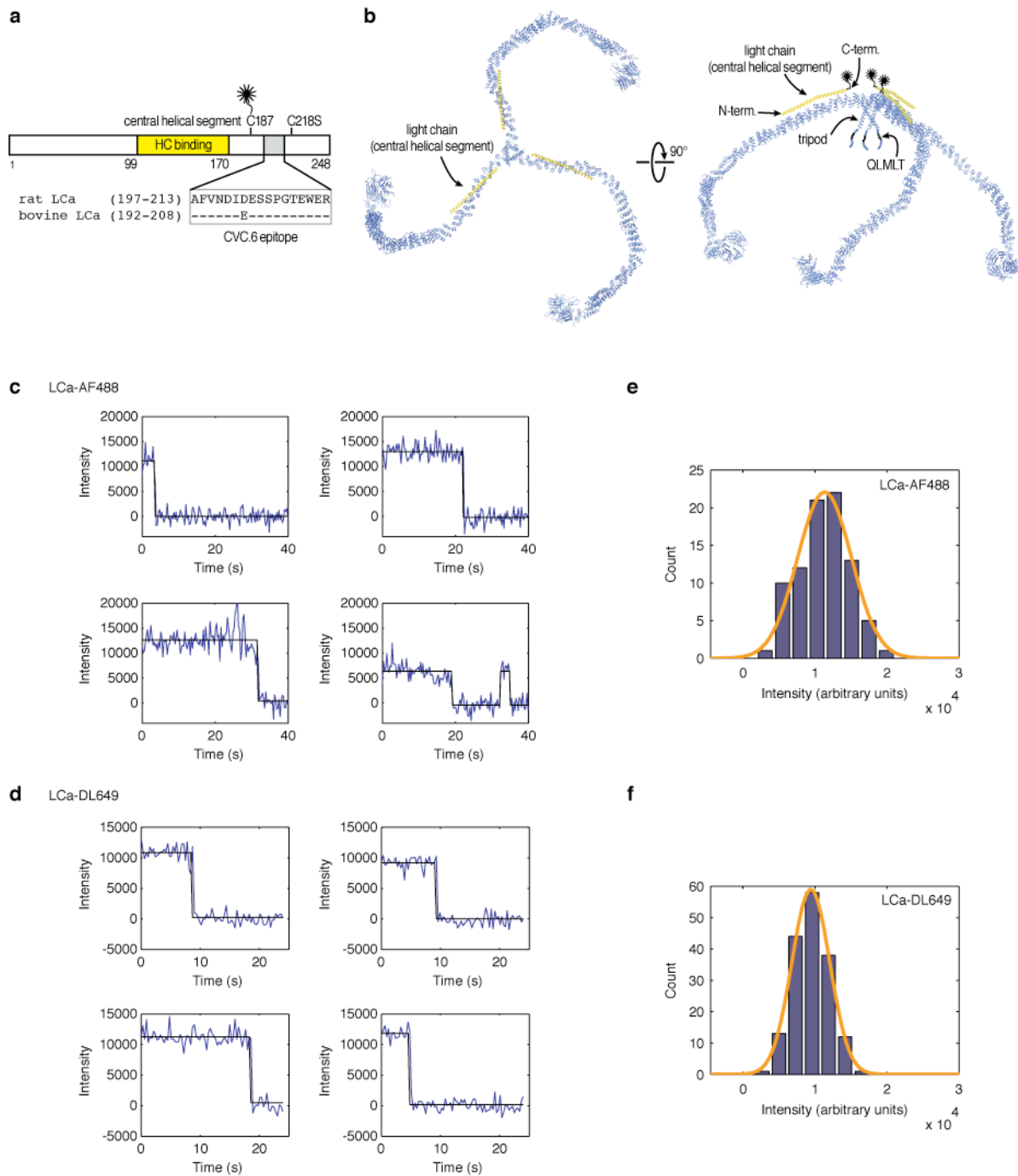
Supplementary Figure 1. Labeling of recombinant clathrin light chain A (LCa) with a single fluorophore. (a) Domain organization of rat clathrin LCa showing the positions of Cys187 used for incorporation of the thiol-reactive fluorophore and the D203E mutation introduced to generate the epitope recognized by the bovine-LCa specific monoclonal antibody CVC.6. **(b)** Top and side views of a clathrin triskelion illustrating the positions of the light chain and the fluorophore. The side view also highlights the location of the tripod and the unstructured heavy-chain C-terminal region, which contains the QLMLT motif recognized by Hsc70. **(c, d)** Single-molecule photobleaching traces of LCa labeled with AlexaFluor 488 (c) or DyLight 649 (d). The data were acquired with TIRF illumination of purified LCa adsorbed to a glass coverslip, using sequential exposures of 300 ms. Single-step photobleaching indicates that the light chain is conjugated to a single fluorophore. **(e, f)** Histogram of single molecule intensities of LCa labeled with AlexaFluor 488 (e) or DyLight 649 (f).

a

b

|	**-ATP**		**+ATP**	
HC release	15%		76%	
	S	P	S	P
HC				
α, β (AP-2)				
Hsc70				
μ2 (AP-2)				
aux 547-910				
LCa				
LCa (AF488)				

c

100 nm

Supplementary Figure 2. Biochemical properties of clathrin/AP-2 coats assembled with recombinant clathrin triskelions containing fluorescently labeled light chain LCa. (a) Model of a D6 clathrin coat, highlighting the positions of the central helical segment of the light chains (yellow) (Reproduced from Fotin, A. et al. *Nature* **432**, 573–9 (2004)). **(b)** Fluorescent coats are uncoated in an auxilin, Hsc70 and ATP dependent manner in ensemble reactions showing that the fluorescent labels do not interfere with coat disassembly. SDS PAGE and Coomassie Blue analysis of the high speed supernatant (S) and pellet (P) fractions of clathrin/AP-2 coats containing LCa–AF488 subjected to a standard uncoating reaction in the presence of auxilin and Hsc70, in the presence and absence of ATP. The percentage of clathrin heavy chain released into the supernatant (HC released) was determined by densitometry of the band corresponding to clathrin heavy chain; the fluorescence image corresponds to the region of the gel containing the labeled clathrin light chain. The ATP dependent disassembly of fluorescent coats is indistinguishable from that of unlabeled coats (Rapoport et al, *Mol Biol Cell* **19**, 405–13 (2008)). **(c)** Image from electron microscopy of a negatively stained (1.2% uranyl acetate) sample of clathrin/AP-2 coats containing fluorescently labeled LCa. The homogeneous appearance of the coats and their size distribution were indistinguishable from D6 barrel coats assembled with unlabeled light chains (Fotin, A. et al. *Nature* **432**, 573–9 (2004); Rapoport et al, *Mol Biol Cell* **19**, 405–13 (2008)). Scale bar: 100 nm.
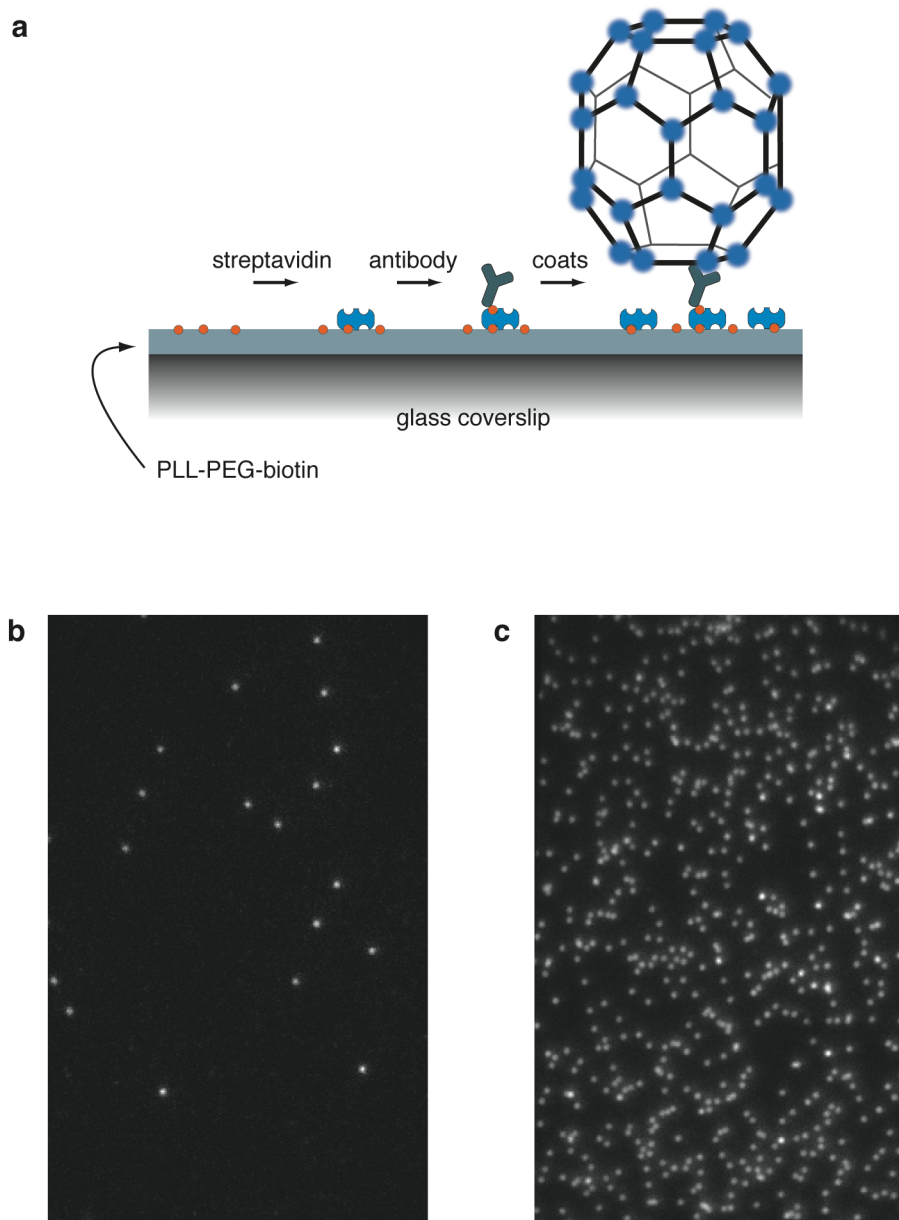
Supplementary Figure 3. Specific capture of clathrin coats onto the modified surface of the glass coverslip. (a) Chemistry for surface functionalization. PLL-PEG-biotin was first adsorbed to a glass coverslip (#1.5), followed by streptavidin and then by the biotinylated monoclonal antibody CVC.6. **(b, c)**. Images acquired by TIRF microscopy of fluorescent clathrin/AP-2 coats that adhered to the glass surface modified with PLL-PEG-biotin and streptavidin in the absence (b) or presence (c) of the CVC.6 monoclonal antibody specific for the bovine clathrin light chain LCa. To determine the level of non-specific binding, the PLL-PEG-biotin/streptavidin surface was exposed to a solution containing 0.1 mg mL^{-1} fluorescent coats (15 μL injection) for 60 s and subsequently rinsed with 200 μL coat formation buffer. Only a few coats adhered non-specifically to the coverslip (b). In contrast, coats were efficiently captured when the antibody was present on the surface (c). A few spots are 2 times brighter than most; they correspond to aggregates of 2 coats and were not included in the analysis.
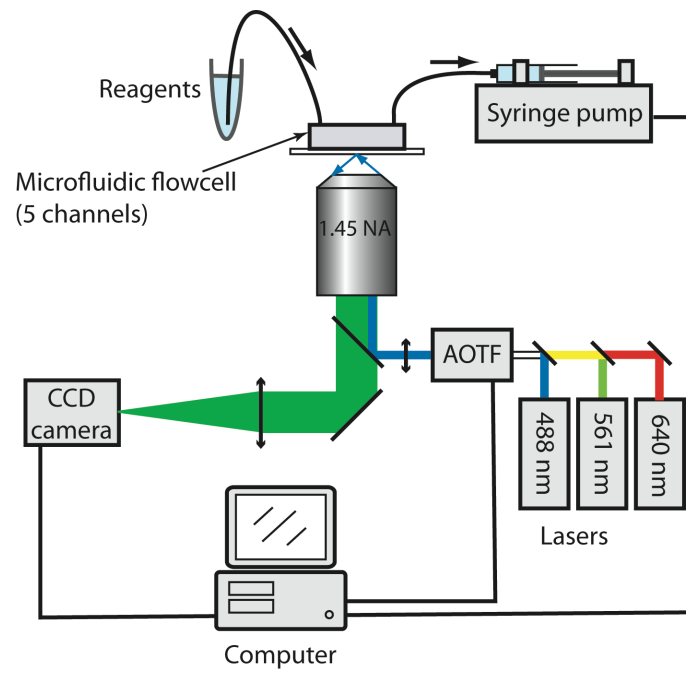
Supplementary Figure 4. Microscope configuration. Schematic representation of the set-up used for the single particle uncoating assay including the components for TIRF microscopy and the microfluidic flow cell.
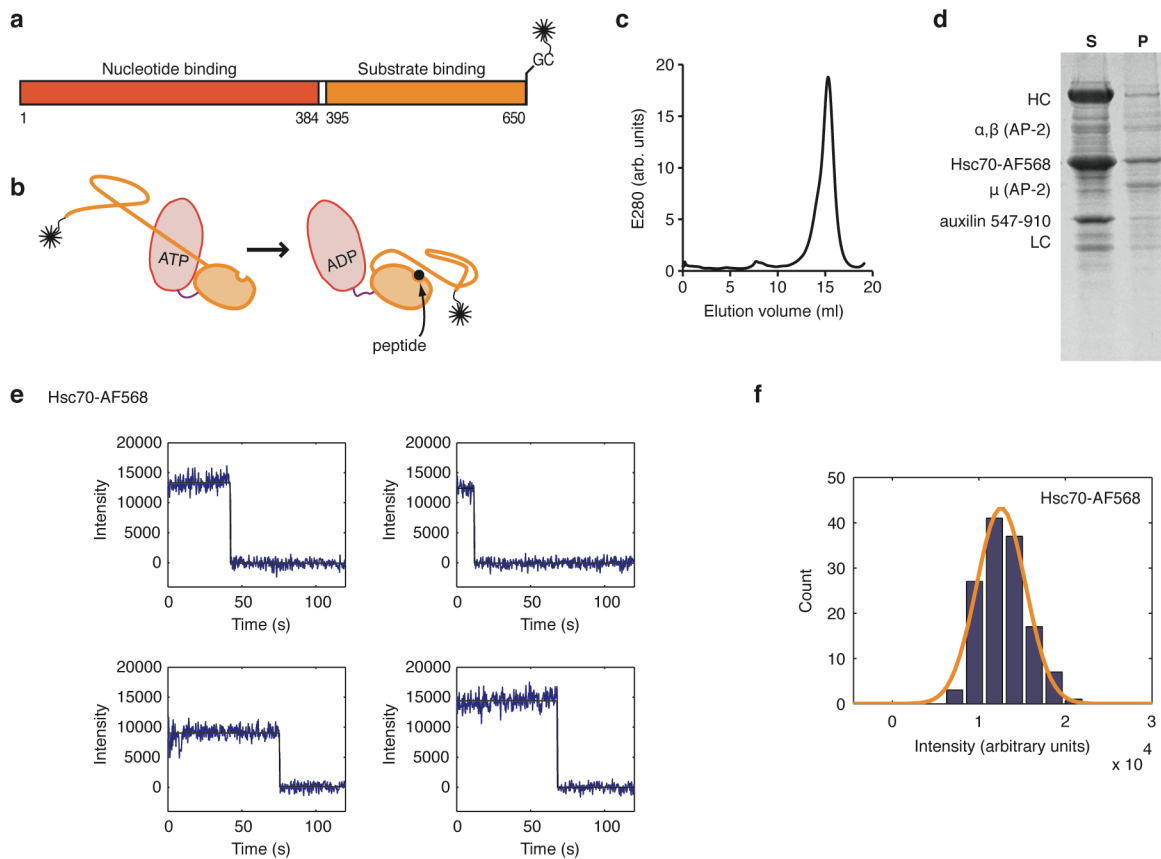
Supplementary Figure 5. Labeling of recombinant Hsc70 with a single fluorophore and verification that the label does not affect its disassembly activity. (a) Domain organization of Hsc70 with glycine and cysteine added to the C-terminus for fluorescent labeling with a thiol-reactive fluorophore. **(b)** Schematic diagram of Hsc70 in the ATP loaded, open conformation and after peptide binding and ATP hydrolysis in the closed conformation (adapted from Liu, Q. & Hendrickson, W.A. *Cell* **131**, 106–20 (2007)). **(c)** Gel filtration elution profile of fluorescently-labeled Hsc70, which elutes as a homogeneous monomer. The chromatography was carried out in 20 mM imidazole, pH 6.8, 100 mM KCl, 2 mM $MgCl_2$ and 0.1 mM ATP. **(d)** SDS PAGE (and Coomassie Blue staining) analysis of the high speed supernatant (S) and pellet (P) fractions of bovine brain clathrin coated vesicles subjected to a standard uncoating reaction in the presence of auxilin, Hsc70-AF568 and ATP (Rapoport et al, *Mol Biol Cell* **19**, 405–13 (2008)). Essentially all of the clathrin was released into the supernatant, confirming that fluorescently labeled Hsc70 remains functional. As expected, minimal amounts of clathrin and AP-2 were released in a control reaction without Hsc70 (not shown). **(e)** Single molecule photobleaching traces of Hsc70 labeled with AF568. The data were acquired with TIRF illumination, using sequential exposures of 300 ms. Single-step photobleaching indicates that the Hsc70 is conjugated with a single fluorophore. **(f)** Histogram of single molecule intensities of Hsc70-AF568.
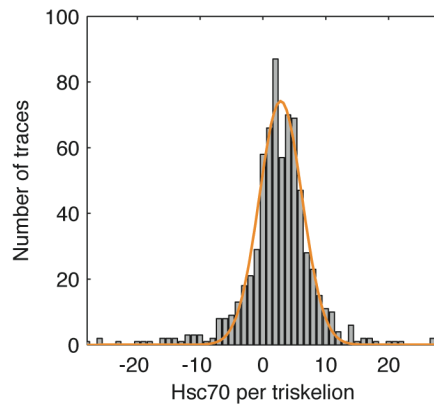
Supplementary Figure 6. Residual Hsc70 at the end of the uncoating reaction. Histogram of the Hsc70 intensity remaining associated with the residual clathrin signal. On average 2.8 (σ = 3.4, N = 705 traces) Hsc70 molecules per triskelion are present at the end of the uncoating reaction. These could occupy up to three QLMLT sites on each of the residual clathrin triskelions(s) attached to surface-immobilized antibody, or some combination of specific and non-specific sites. Binding of more than one Hsc70 to specific (QLMLT) sites on the residual triskelions is possible, because removal of neighboring triskelions has eliminated steric hindrance from their ankle segments.
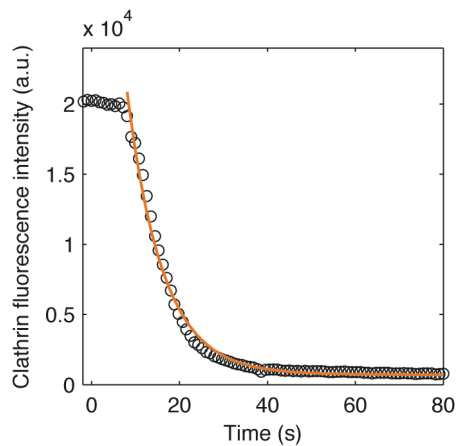
**Supplementary Figure 7. Analysis of the disassembly reaction from the single particle uncoating assay as an ensemble reaction.** Representative "ensemble" uncoating trace, calculated by averaging all disassembly traces recorded in the single particle uncoating assay using 2 μM Hsc70 (N = 621 coats). The ensemble half life (6 s) was calculated by a fitting single exponential to the averaged intensity decay (orange line).
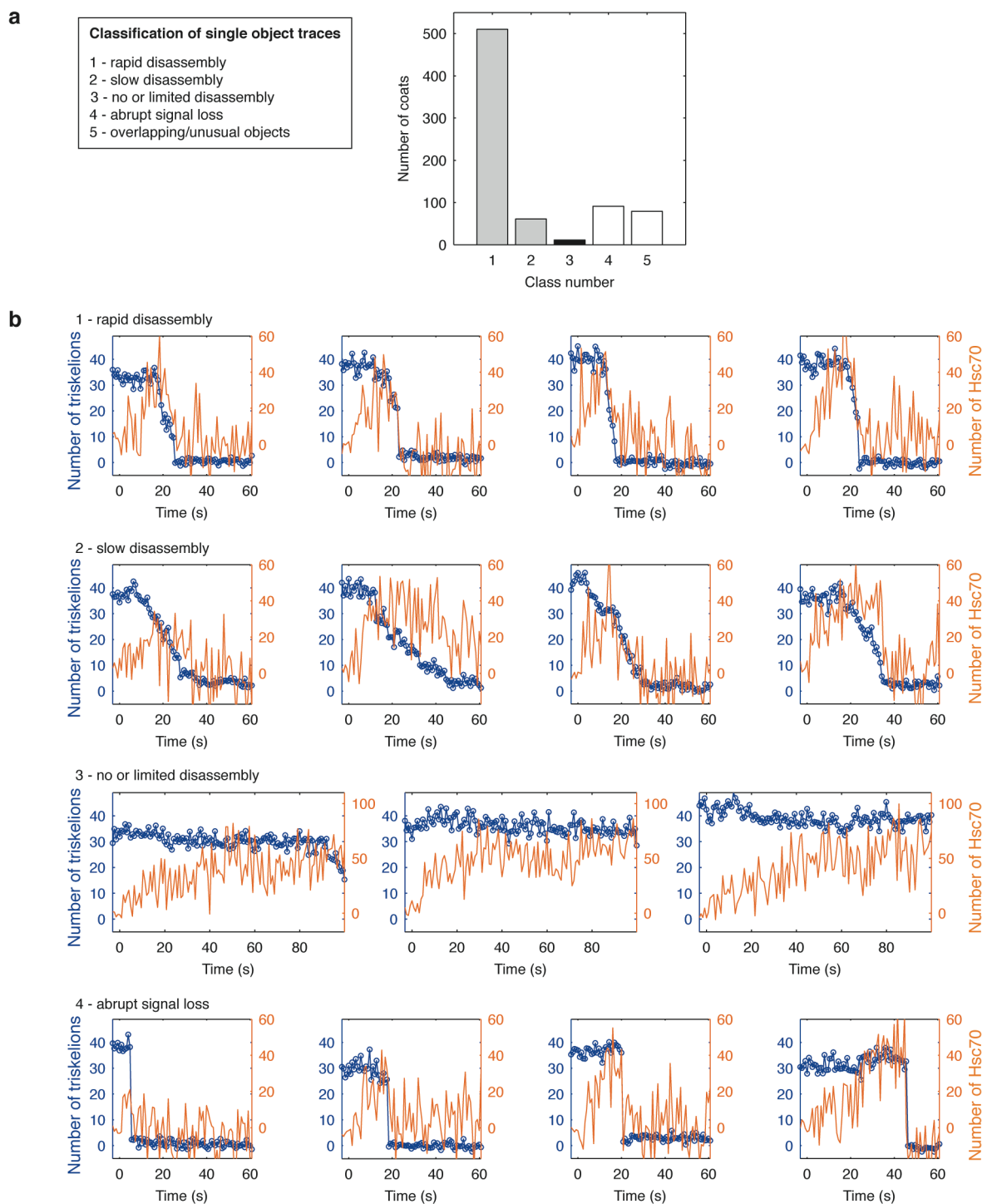
Supplementary Figure 8. Classification of fluorescence traces from the single-particle uncoating assay. (a) Classes of traces and their distribution among the different classes. The data are from a single uncoating experiment with 1.2 μM Hsc70. **(b)** Examples of traces illustrating the different classes. The majority of traces showed a rapid disassembly phase (class 1), while disassembly of some coats was comparatively slow (class 2). At high Hsc70 concentrations (≥ 0.9 μM) only a small fraction (< 5%) of the coats failed to disassemble (class 3). Residual clathrin remaining on the surface at the end of the uncoating experiment was ≤1 triskelion for 40% of coats, ≤3 triskelions for 80% of the coats and ≤6 triskelions for 95% of the coats. The abrupt disappearance of the coat signal within a single frame (class 4) may represent the dissociation of the entire coat from the surface and could therefore not be interpreted unambiguously as uncoating. These objects and those with overlapping point-spread functions were excluded from further analysis.
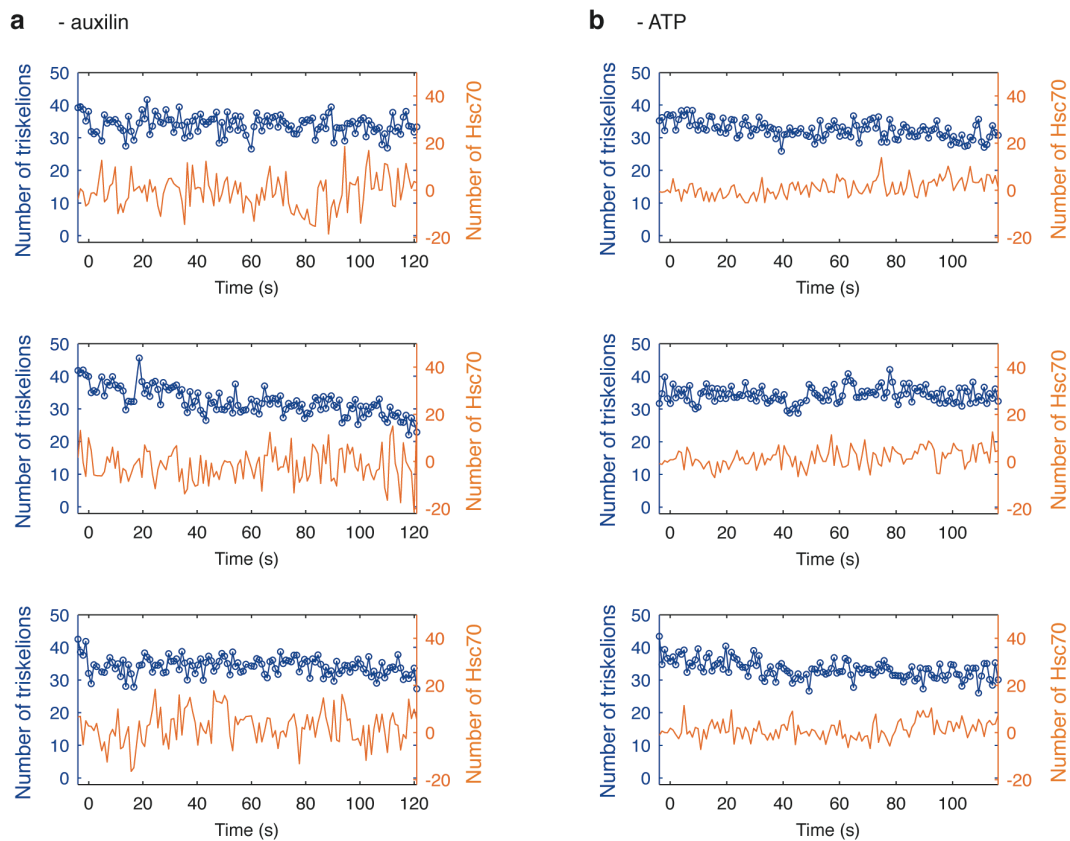
Supplementary Figure 9. Effects of omitting auxilin or ATP. (a) Representative clathrin (blue) and Hsc70 (orange) traces of coats subjected to the single particle uncoating assay using 1 µM Hsc70 in the absence of auxilin. Under these conditions 94% of the coats remained intact ($N = 717$ coats). **(b)** Representative clathrin (blue) and Hsc70 (orange) traces of coats subjected to the single particle uncoating assay using 1 µM Hsc70 in the absence of ATP. The reaction mixture containing Hsc70 and auxilin was incubated with glucose (10 mM) and hexokinase (20 units mL^{-1}) for 7 minutes at room temperature to remove residual ATP prior to injection into the flow cell. Under these conditions 97% of the coats remained intact ($N = 604$ coats). During imaging we observed an increased number of Hsc70 aggregates as expected in the absence of ATP. Non-hydrolysable ATP analogs do not substitute for ATP in recruitment of Hsc70 by auxilin, nor do the transition-state analogs, ADP-AlF^{-4}, ADP-BeF^{-3} and ADP-V$_i$. Moreover, Hsc70, which is monomeric when loaded with ATP, self-associates in the presence of ATP-γ-S or AMP-PNP.
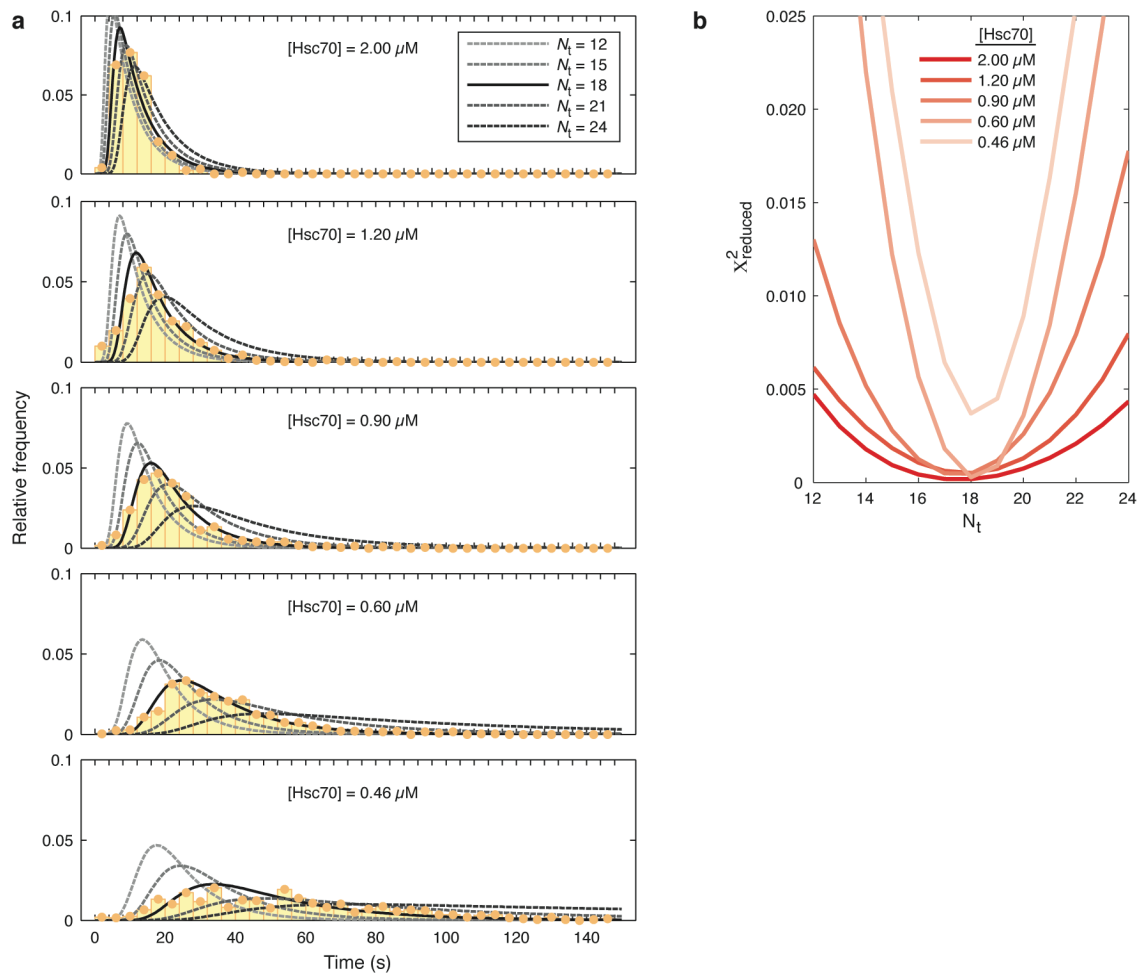
Supplementary Figure 10. Number of Hsc70 molecules required to initiate uncoating. (a) Fit of the kinetic model to the accumulation-time distributions. This calculation provides a robust and concentration independent estimate for the number of Hsc70 molecules required to initiate uncoating (N_t). Fitting the observed accumulation time distributions (histograms) for various Hsc70 concentrations yields an estimate of $N_t = 18$ (solid black line). The model diverges rapidly from the observed accumulation time distribution when N_t is altered (shown for $N_t = 12, 15, 18, 21$ and 24, dashed greyscale lines). **(b)** Reduced X^2 between the empirical cumulative distributions of the measured accumulation times and the cumulative distribution function from the model determined for each Hsc70 concentration. The same global minimum at $N_t = 18$ obtained for each concentration confirms the accuracy of the model.
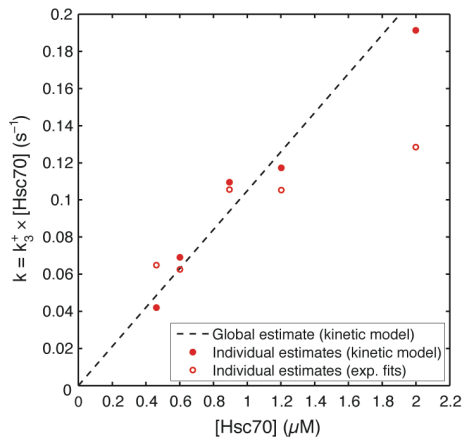
Supplementary Figure 11. The rate of coat disassembly depends linearly on Hsc70 concentration. Estimates of the rate constant k_3^+ were obtained by fitting the kinetic model to the full uncoating time histograms and by fitting an exponential to the disassembly time histograms (disassembly times were obtained by taking the difference between the detected association and uncoating times, which results in a noisier estimate). The rate k_3^+ = 0.1050 μM^{-1} s^{-1} was obtained from a global fit of the kinetic model over all Hsc70 concentrations.
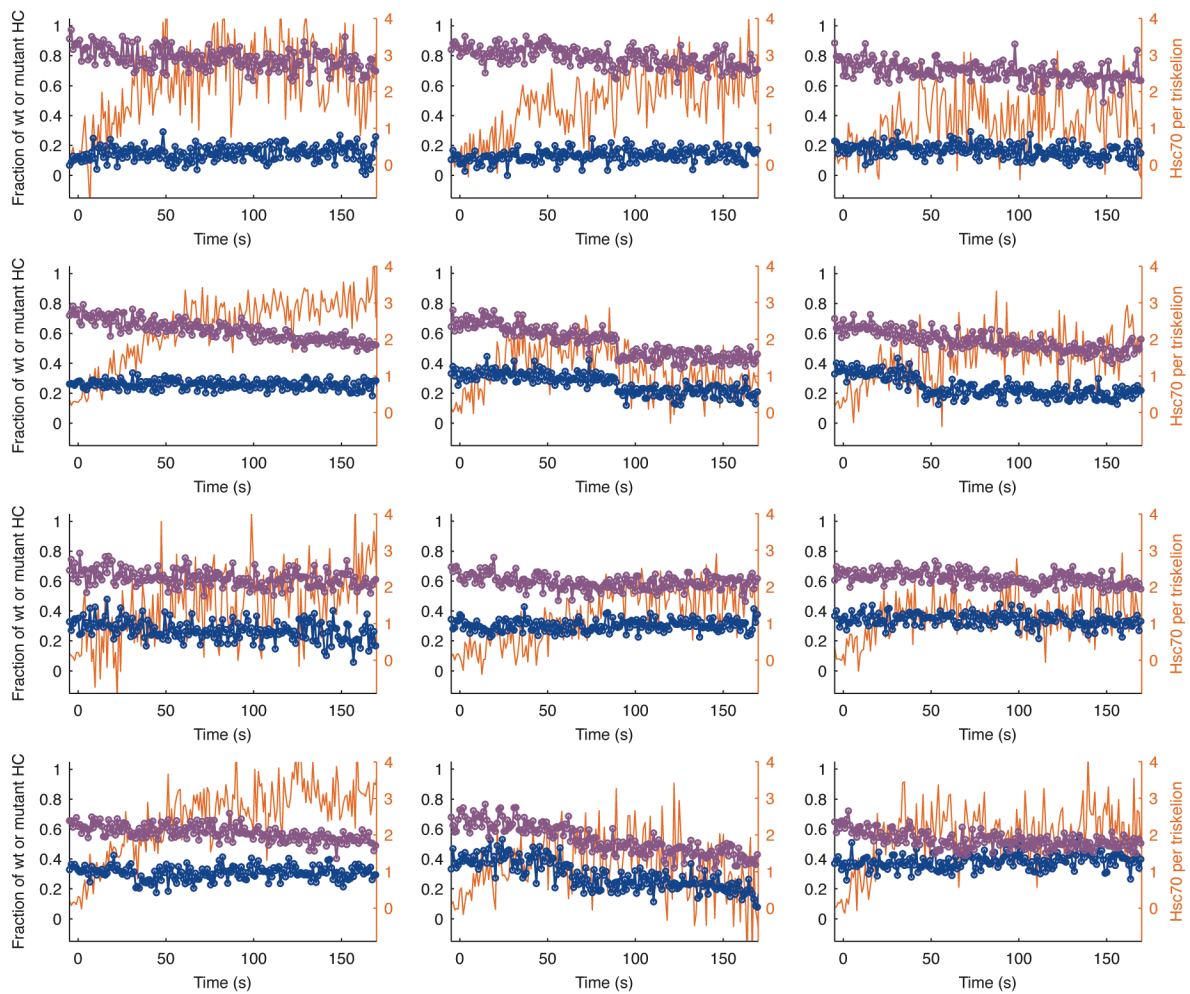
Supplementary Figure 12. Mixed coats containing an excess of mutant clathrin do not undergo Hsc70-driven uncoating. Additional examples of traces from coats containing mixtures of wild type and truncated clathrin in the single-particle uncoating assay; blue, wild-type clathrin; purple, mutant clathrin; orange, Hsc70. Wild-type clathrin is not removed selectively from coats that fail to disassemble.

SUPPLEMENTARY METHODS

Labeled recombinant clathrin. Wild-type rat clathrin heavy chain and a mutant truncated at residue 1637 (and hence lacking the Hsc70-binding motif Q_{1638}LMLT) were expressed in insect cells and purified as described (Rapoport et al, *Mol Biol Cell* **19**, 405–13 (2008)). The purified clathrin was stored frozen at -80 °C in the presence of 20% glycerol.

cDNA encoding rat clathrin light chain a1 (LCa) was cloned into the pET28 expression vector using the Nco I and EcoR I restriction sites to allow expression without a poly-histidine tag. The following point mutations were introduced by site-directed mutagenesis (Supplementary Figure 1): (1) D203E, to restore the epitope present in bovine clathrin LCa recognized by the monoclonal antibody CVC.6 and (2) C218S, to remove one of the two cysteines in the light-chain sequence and thus allow site specific labeling at C187 with thiol-reactive reagents. LCa was expressed in *E. coli* strain BL21(DE3) grown in LB medium containing 30 mg L^{-1} kanamycin at 37 °C with shaking (250 rpm) to an optical density of 0.5. After induction with 0.6 mM IPTG and expression for 3 h at 37 °C, the cells were harvested by centrifugation (Sorvall RC3B rotor, 5000 rpm, 10 min, 4 °C) and resuspended in ice-cold lysis buffer (20 mM BisTris, adjusted to pH 6.0 at room temperature, 0.5 mM dithiothreitol (DTT), 1 mM EDTA, "Complete" protease inhibitor cocktail (Roche Applied Science)) using 20 mL lysis buffer per 3.5 g wet cell weight. The suspension was introduced into a glass conical flask, which was immersed in boiling water for 5 min and then chilled on ice. Precipitated material was removed by centrifugation (Beckman 60Ti rotor, 54000 rpm, 30 min, 4 °C), and LCa was purified from the filtered supernatant (0.2 μm syringe filter) by anion exchange chromatography at 4 °C using a HiTrap MonoQ column (1 mL, GE Life Sciences) equilibrated with buffer A (20 mM BisTris adjusted to pH 6.0 at room temperature, 0.5 mM DTT). LCa was eluted with a linear gradient from 0% to 32% buffer B (20 mM BisTris adjusted to pH 6.0 at room temperature, 0.5 mM DTT, 1 M NaCl) and the eluted protein dialyzed against labeling buffer (20 mM Tris pH 7.4, 1 mM EDTA, 0.2 mM tris(2-carboxyethyl) phosphine (TCEP)).

To introduce a fluorescent label at C187 of LCa, a maleimide functionalized dye was added to the protein solution (3–6 mg mL^{-1}) with a molar excess between 4:1 - 8:1 and allowed to react for 2 hours at room temperature. The unreacted dye was quenched with 2-mercaptoethanol added to a final concentration of ~10 mM. Most of the free dye was removed by 10-fold dilution of the reaction mixture with buffer A (without DTT) followed by concentration in a centrifugal filtration device (Millipore, MWCO 10 kDa). This procedure was repeated until the flow-through was almost colorless. The labeled light chain was further purified by anion exchange chromatography at 4 °C on a HiTrap MonoQ column (1 mL, GE Life Sciences) equilibrated with buffer A and eluted with a linear gradient from 0% to 65% buffer B (without DTT) over 40 column volumes. The purified labeled light chain was stored frozen at -80 °C in the presence of 20% glycerol.

For *in vitro* reconstitution of fluorescent clathrin, recombinant heavy-chain trimers were mixed with excess labeled LCa at a molar ratio of HC:LC of 1:2.4 and incubated for 40 min at room temperature just prior to coat assembly. To determine the number of dye molecules incorporated per triskelion, we separated reconstituted clathrin (HC+LC) from free light chain by inducing the formation of clathrin cages and harvesting the cages by high speed centrifugation (Rapoport et al, *Mol Biol Cell* **19**, 405–13 (2008)). The cages were resuspended in 100 mM Tris pH 7.5, and protein and fluorescent-label concentrations were determined by UV-visible absorption spectroscopy. More than ~96% of the heavy chains were occupied with a labeled light chain.

Recombinant auxilin. The C-terminal fragment of bovine auxilin (residues 547–910) containing the clathrin-binding and J-domain functions was expressed as a GST-fusion protein in *E. coli* and purified as described previously (Rapoport et al, *Mol Biol Cell* **19**, 405–13 (2008)). Briefly, the fusion protein was isolated by affinity chromatography followed by removal of the GST tag by thrombin cleavage. The auxilin fragment was further purified using cation exchange chromatography, dialyzed against uncoating buffer containing 20% glycerol, and stored frozen at -80 °C.

Labeled recombinant Hsc70. cDNA encoding bovine Hsc70 was introduced into the pProEX HTc vector for expression as a fusion protein with an N-terminal, TEV cleavable His-tag. The C-terminus of Hsc70 was modified for site-specific labeling by adding a glycine and a cysteine residue (Supplementary Figure 5a and b). The fusion protein was expressed in *E. coli* strain BL21-DE3. The bacteria were grown at 37 °C in 2 × 600 mL LB medium containing 30 mg L^{-1} kanamycin to an O.D. of 0.3, then transferred to 16 °C and grown to an O.D. of 0.4. Protein expression was induced by addition of IPTG to a final concentration of 0.1 mM. The induced cells were grown overnight at 16 °C, harvested by centrifugation, resuspended in 25 mL lysis buffer [50 mM Tris HCl pH 7.5, 300 mM NaCl, "Complete" protease inhibitor cocktail (Roche Applied Science)], and disrupted by shearing using a laboratory model microfluidizer (Microfluidics, Newton MA). After removing the cell debris by centrifugation (Beckman Type 45 Ti rotor, 40000 rpm, 4 °C, 45 min), the fusion protein was isolated by immobilized metal affinity chromatography on Co beads (3 mL bed volume, Talon resin, Clontech). After a 2 hr incubation with the preparation at 4°C, the beads were washed with 15 mL lysis buffer followed by a pre-elution step with 15 mL lysis buffer containing 10 mM imidazole. The His-tagged protein was eluted with 20 mL lysis buffer containing 80 mM imidazole and collected in 0.5 mL fractions. EDTA and DTT were added to the eluted protein at final concentrations of 2 mM. The N-terminal His-tag was removed by digestion with TEV protease at room temperature for 5 hours. The sample was then dialyzed against lysis buffer (dialysis tubing, MWCO 10–12 kDa) and undigested fusion protein removed by binding to Co beads (0.5 mL bed volume, Talon beads, Clontech) as described above. The flow-through containing only cleaved protein was collected, and 0.1 mM TCEP, 1 mM $MgCl_2$ and 0.1 mM ATP (final concentrations) were added. The solution was concentrated using a centrifugal filtration device (Millipore Amicon Ultra-4, 30 kDa MWCO) and centrifuged to remove aggregates (Eppendorf F45-30-11 rotor, 14000 rpm, 4 °C, 10 min). The final Hsc70 yield was 12 mg (~5 mg mL^{-1}).

Preferential labeling at the C-terminal cysteine residue of Hsc70 was achieved by addition of the thiol-reactive fluorophore AlexaFluor-C5-maleimide (5:1 fluorophore:protein, mol/mol) for 80 min at room temperature. After quenching of the unreacted fluorophore with 2-mercaptoethanol (final concentration of ~20 mM), the labeled Hsc70 was separated from the free fluorophore by gel filtration on a Superose 6 HR 10/30 column (Amersham Biosciences) operated at 0.5 mL min^{-1} with a buffer containing 20 mM imidazole adjusted to pH 6.8, 100 mM KCl, 2 mM $MgCl_2$ and 0.1 mM ATP. The fractions containing labeled Hsc70 were combined, concentrated by centrifugal ultrafiltration as described above, flash-frozen in liquid nitrogen after addition of 20% glycerol and stored at -80 °C. The labeling yield of the reaction determined using UV-visible absorption spectroscopy was ~97%.

As a control for labeling specificity, wild-type, full-length Hsc70 (without C-terminal cysteine) was treated with a ten-fold molar excess of a thiol-reactive fluorophore (AF568-C5-maleimide) at room temperature for 150 minutes. The wild-type Hsc70 did not incorporate an appreciable amount of label, demonstrating that the four cysteine residues of the enzyme are not accessible for modification and that reaction of the thiol-reactive label with other nucleophilic groups was negligible under the conditions used.

Gel filtration chromatography showed that in the presence of ATP, the labeled Hsc70 is monomeric (Supplementary Figure 5c). The labeled enzyme had normal activity when used as a disassemblase in a conventional ensemble uncoating assay with clathrin/AP-2 coats as substrate, as shown by the efficient release of clathrin into the high-speed supernatant fraction (Supplementary Figure 5d).

Coat formation. The tetrameric clathrin adaptor complex AP-2 was purified from coated vesicles isolated from calf brain as described (Boll, W. et al, *EMBO J* **15**, 5789–95 (1996); Gallusser, A. & Kirchhausen, T. *EMBO J* **12**, 5237–44 (1993)). Contaminating auxilin was removed by using a final hydroxylapatite chromatographic step (Rapoport, I. et al, *Mol Biol Cell* **19**, 405–13 (2008)). Fluorescent clathrin triskelions were mixed with AP-2 at a ratio of 3:1 w/w) and dialyzed at 4 °C in the dark overnight against coat formation buffer (50 mM MES pH 6.5, 100 mM NaCl, 2 mM EDTA, 0.5 mM DTT) followed by an additional 4–6 h dialysis. After removal of small amounts of aggregated material by low speed centrifugation (TLA 100.4 rotor, 12000 rpm, 10 min, 4 °C), the coats were isolated by high speed centrifugation (TLA 100.4 rotor, 65000 rpm, 14–16 min, 4 °C) and resuspended at room temperature in coat formation buffer at a concentration of ~ 1 mg mL^{-1}.

Coats assembled with labeled or unlabeled recombinant clathrin were indistinguishable from each other in clathrin/AP-2 composition, appearance by electron microscopy and in their auxilin-, Hsc70- and ATP-dependent disassembly in the ensemble uncoating assay (Supplementary Figure 2). Coats stored at 4 °C were used for disassembly experiments within 5 days of preparation. Prolonged storage led to a reduced uncoating efficiency. Alternatively, coat samples containing 20% glycerol were frozen in liquid nitrogen and stored at -80 °C. The uncoating kinetics of these coats in the single particle uncoating assay were the same as those of freshly prepared material.

Coats containing mixtures of wild type triskelions (reconstituted with LCa–AF488) and mutant triskelions (reconstituted with LCa–DL649) were assembled after combining the labeled wild-type and mutant triskelions in various molar ratios with AP-2. The composition of the resulting coats was established by capturing them on the modified glass coverslip and determining in each coat the relative fluorescence intensities of the AF488 and DL649 fluorophores by TIRF imaging. Analysis of coats assembled using a 1:1 molar ratio revealed random incorporation of the wild type and mutant triskelions coats (normal distribution of wild type content ~50±7 %, mean±std, n = 404 coats). The range of compositions was extended by using coats prepared from mixtures containing 25%, 45%, 65% and 85% wild-type clathrin in the single particle uncoating assay. The wild type clathrin content of these coats ranged from ~5% to ~95%.

Surface preparation for specific capture of coats by the glass coverslip. Glass coverslips (#1.5, Warner Instruments, Hamden, CT) were cleaned by sonication in filtered ethanol for 30 min

followed by sonication in filtered 1 M aqueous NaOH for 30 min using a bath sonicator (Branson). The coverslips were rinsed by multiple immersions in deionized Milli-Q water, each time breaking the air-water interface. The entire sonication and rinsing procedure was repeated once. The coverslips were then dried at 120 °C and exposed to an air plasma inside a glow discharge unit operated at 50 mA for 2–3 min (Electron Microscopy Sciences). The freshly cleaned coverslips were modified by adsorption of a co-polymer composed of poly-L-lysine (PLL) and biotinylated poly(ethylene glycol) (PEG) (Susos AG, PLL(20)-g[3.4]-PEG(2)/PEG(3.4)-biotin (20%)) in PBS (1 mg mL^{-1}). A drop of this solution (60 µL) was sandwiched between two coverslips and incubated in a humid chamber at room temperature for 30–60 min. The modified coverslips were then rinsed with copious amounts of deionized water and stored dry under reduced pressure for up to two weeks.

Just before assembly of the microfluidic flow cell, the modified coverslips were covered with a solution of streptavidin (100 µL, 0.2 mg mL^{-1}, Sigma-Aldrich) in blocking buffer (20 mM Tris pH 7.5, 2 mM EDTA, 50 mM NaCl, 0.03% NaN$_3$, 0.025% Tween 20, 0.2 mg mL^{-1} BSA), incubated at room temperature in a humid chamber for 30 min and rinsed with deionized water.

Preparation and assembly of the microfluidic flow cell. The flow cell was prepared by pressing a PDMS device with microfluidic flow channels (800 µm width, 80–100 µm height) onto the dry streptavidin modified coverslip. The PDMS device was prepared using standard protocols for soft lithography. The conformal seal formed between the PDMS and the glass surface is sufficient to avoid leakage of solution (or air) between channels. The flow cell was clamped into a custom-made stainless steel holder designed to fit onto the sample holder on the microscope stage. Solutions were drawn through the channel via tubing with a programmable syringe pump (PHD 22/2000, Harvard Apparatus) operating in the refill mode. The inlet tubing was kept short (~ 5 cm) and had a low internal diameter (0.2 mm) to minimize the dead volume before the channel was reached.

Capture of fluorescent clathrin coats onto the surface of modified coverslips. The monoclonal antibody CVC.6, which recognizes an epitope located in the C-terminal region of bovine clathrin LCa, was biotinylated using the amine reactive reagent biotin-XX-sulfosuccinimidyl ester (Molecular Probes) by adding 10 µL of a 1M NaHCO$_3$ solution to 100 µL of CVC.6 in PBS (1.6 mg mL^{-1}) to raise the pH, followed by 1.3 µL of a freshly prepared 15 mM solution of the biotinylation reagent. The mixture was incubated at room temperature for 45 minutes, dialysed against PBS containing 0.05% NaN$_3$ and stored at 4 °C. The degree of biotinylation was determined as ~10 biotin per antibody using the [2-(4′-hydroxyazobenzene) benzoic acid] (HABA) assay (Pierce). The biotinylated antibody CVC.6 was immobilized on the surface of the PLL/PEG coverslip coated with streptavidin by flowing 8–12 µL of a solution containing the antibody (~2.5 µg mL^{-1} in blocking buffer) through the flow channel at a flow rate of 3 µL min^{-1}. After rinsing the channel with coat formation buffer, 1–2 µL of a solution containing fluorescent coats (~ 0.1 mg mL^{-1}) was passed through the channel, immediately followed by 20 µL of coat formation buffer at a flow rate of 0.05 mL min^{-1}. Typically, between 600 to 1400 coats per field of view (~ 40 µm × 40 µm) bound to the surface during this brief exposure to the coat solution.

Imaging. A schematic of the microscope configuration is shown in Supplementary Figure 4. Data were collected on a Mariana™ system (Intelligent Imaging Innovations, Denver CO), based on a 200M inverted microscope and TIRF slider with manual angle and focus controls (Zeiss). Images were acquired with an oil immersion Alpha Plan-Apo 100× objective (1.46 NA). Solid state lasers were used for excitation at wavelengths of 488 nm (Saphire, 50 mW, Coherent Inc.), 561 nm (Jive, 50 mW, Cobolt AB) and 640 nm (Cube, 40 mW, Coherent Inc.). The excitation light was coupled through an acousto-optical tunable filter into a single mode fiber optic, carried to the TIRF slider and reflected into the objective using a multi-band dichroic mirror (Di01-R405/488/561/635, Semrock). Fluorescence emission light collected by the objective passed the dichroic mirror and a multi-band emission filter (FF01-446/523/600/677, Semrock). A spherical aberration correction unit (Intelligent Imaging Innovations) was inserted into the emission path. Images were acquired with an electron multiplying charge coupled device (EMCCD) camera (QuantEM, Photometrics). Microscope operation and image acquisition were controlled using SlideBook software (V4.2.12, Intelligent Imaging Innovations).

Images were acquired sequentially for each wavelength using exposures in the range of 2–10 ms and a dwell time of ~ 70 ms for transfer of each image to the RAM of the computer. The frame rate was generally limited to 1–2 Hz for experiments in which uncoating was monitored over a period of 2 or more minutes, in order to prevent photo-cross-linking of the proteins within the coat. We observed that prolonged exposure or imaging at higher frame rates leads to a gradual loss of uncoating competence.

The angle of incidence of the excitation light onto the coverslip/buffer interface was adjusted to generate an evanescent field (estimated penetration depth between 200–300 nm) sufficient to excite the fluorophores associated with the coat (dimensions of a D-6 barrel coat: 728 × 670 Å) while avoiding excessive background fluorescence in the red channel after injection of the uncoating reagents. Under these conditions the fluorophores at the top of the coat are excited with ~70–80% of the power illuminating those at the bottom of the coat (close the coverslip).

Single-particle fluorescence imaging uncoating assay. To improve the photostability and photophysics of the fluorescent dyes, all imaging buffers contained the vitamin E derivative Trolox (2 mM), and DTT was absent. Photostability of clathrin light chain labeled with AlexaFluor 488 and of Hsc70 labeled with AlexaFluor 568 did not improve appreciably in the presence of an oxygen quenching system. In contrast, inclusion of the protocatechuic acid/protocatechuate-3,4-dioxygenase system (Aitken, C.E. et al, *Biophys J* **94**, 1826–35 (2008)) slowed the comparatively rapid photobleaching of light chain labeled with DyLight649.

Immediately after capture of the clathrin/AP-2 coats onto the surface of the modified coverslip, auxilin was added by flowing 24 µL of a solution of 0.05 mg mL^{-1} auxilin in uncoating buffer (20 mM imidazole pH 6.8, 100 mM KCl, 2 mM MgCl$_2$) through the microfluidic channel at a flow rate of 8 µL min^{-1}. The uncoating reaction was initiated by introducing 20–30 µL of a reaction mixture containing Hsc70-AF568 at various concentrations, 0.02 mg mL^{-1} auxilin and 2 mM ATP in uncoating buffer at a flow rate of 0.1 mL min^{-1} to allow rapid solution exchange (achieved within 2 s). The flow rate was then decreased to 0.01 mL min^{-1} for the remainder of the experiment.

One of the experiments was designed to obtain an independent estimate of the rate constant k_2^+ associated with the final step in the kinetic model (Figure 6a), using conditions that separate the

step constituting the Hsc70 association phase from the entry into the disassembly phase. Coats were first stabilized while binding auxilin and Hsc70–ATP by incubation at pH 6.0 (Xing, Y. et al. *EMBO J* **29**, 655–65 (2010)). and then shifted to pH 6.8 to trigger the uncoating reaction (Figure 7). Clathrin coats were loaded for 5–10 min with auxilin (0.05 mg mL^{-1}) and Hsc70-AF568 (0.25 mg mL^{-1}) in low pH buffer (20 mM MES pH 6.0, 100 mM KCl, 2 mM MgCl$_2$). Under these conditions the coats remain intact with no decrease of the clathrin fluorescence signal. Uncoating was triggered upon increasing the pH by flowing uncoating buffer (pH 6.8) containing auxilin, unlabeled Hsc70 and ATP into the flow channel. When the pH shift was carried out in the absence of Hsc70, uncoating was largely prevented due to the rapid dissociation of bound Hsc70 from the coats.

Image analysis. Images were analyzed with software written in MATLAB (The MathWorks, Inc.). Out-of-focus frames due to stage drift were removed from movies before analysis. Clathrin/AP-2 coats appear as diffraction limited objects and were detected as local maxima in an averaged fluorescence image (average of the first five frames collected before addition of uncoating reagents), corrected for unevenness in illumination. The positions of the coats were then determined by calculating the mean adjusted center of intensity at each local maximum. Overlapping objects (non-diffraction limited objects) were excluded from analysis. Fluorescence traces were calculated by Gaussian fitting of the signals in each channel. These traces were very similar to those determined by integrating the fluorescence intensity in a 5×5 or 7×7 pixel region for each channel. The fluorescence intensity for each object was corrected for background fluorescence, determined from 500 background pixels in the vicinity of the object. Background pixels were defined using a mask that excludes bright objects from the time series.

Fluorescence traces were sorted into classes: (1) uncoating traces with a phase of rapid signal disappearance, (2) traces with a phase of slow signal disappearance and (3) traces with no decrease (or only limited decrease) in the intensity over the duration of the entire experiment. Classification was automated by determining whether a trace fell below an intensity threshold and whether it exhibited a sharp minimum when transformed with a first order Savitzky-Golay differentiation filter (time derivative trace). The automated classification was verified and refined manually. Traces showing a disappearance of the entire signal within a single frame were interpreted as the release of the coat from the modified coverslip and therefore excluded from analysis. Uncoating efficiency in Fig 3, 4 and 8 is defined as the percentage of traces with a phase of rapid signal disappearance (class 1).

Arrival of the uncoating reagents was detected as an overall increase of the background fluorescence in the red channel (~2 s). Accumulation times (defined as the time between arrival of the reagent and initiation of the phase of rapid signal disappearance) were determined for each trace using an algorithm based on the automated step-fitting method provided by J. Kerssemakers and M. Dogterom (AMOLF, Amsterdam, Netherlands) (Kerssemakers, J.W.J. et al. *Nature* **442**, 709–12 (2006)).

The relative fluorescence intensities of the single fluorophores (AF488, AF568 and DL649) were determined from the quantal photobleaching step in single-molecule photobleaching traces of each of the labeled proteins continuously imaged in uncoating buffer, using exposure times between 20 and 300 ms per frame. The measurements were done with the same settings of the CCD camera as in the uncoating experiments but with longer exposure times, required because the short exposures used to image coats result in low signal-to-noise ratios in the single-flurophore

fluorescence, preventing reliable determination of the photobleaching step. We verified the linearity of the procedure and further calibrated the results by ensuring that the number of triskelions 'counted' in a coat corresponded to 36, the number of triskelions assembled in the D6-barrel coats used for the uncoating study. The samples were prepared by adsorbing the labeled protein onto the surface of a clean glass coverslip (~ 40 pM in PBS containing 180 nM bovine serum albumin, supplemented with 0.1 mM ATP for Hsc70) for 5 min, followed by rinsing with PBS.

The number of Hsc70 molecules bound per triskelion at the initiation of coat disassembly was determined from the ratio of the Hsc70 fluorescence intensity (determined from the Hsc70 trace smoothed by a moving average filter with a window size of 5 frames) at the tie point at which disassembly begins to the clathrin-coat fluorescence intensity before addition of uncoating reagents. Only coats that disassembled within the mean disassembly time of the entire population were used for this analysis. Photobleaching was minimal within the imaging interval, and therefore no correction was made. The relative intensities of the fluorophores used to label clathrin and Hsc70 (see below) were taken into account to calculate the Hsc70:clathrin molar ratio.

Kinetic model

Estimation of Hsc70 association and dissociation rate constants. Hsc70 association and dissociation rates for an individual coat were determined by fitting a binding equation of the form

$$I_{[\text{Hsc70}]}(t) = A_0 \frac{k_1^+[\text{Hsc70}]}{k_1^+[\text{Hsc70}] + k_1^-}\left(1 - \mathrm{e}^{-(k_1^+[\text{Hsc70}] + k_1^-)t}\right) \quad (1)$$

to the set of all measured traces, at various concentrations. $A_0 \dfrac{k_1^+[\text{Hsc70}]}{k_1^+[\text{Hsc70}] + k_1^-}$ corresponds to the

fluorescence intensity at Hsc70 saturation (in arbitrary units), and k_1^+ and k_1^- are the microscopic rate constants for association and dissociation at a single site. The order of the rate constant k_1^+ was first estimated by fitting binding equations at individual concentrations, which yielded a linear dependence on concentration (data not shown); the results of the global fit are shown in Figure 5. The estimated values for the average behavior were $k_1^+ = 0.070\ \mu\text{M}^{-1}\text{s}^{-1}$ and $k_1^- = 0.027\ \text{s}^{-1}$, respectively.

We also determined the dissociation rate constant directly by following dissociation of Hsc70-AF568 from stabilized coats. To maintain coat stability during Hsc70-AF568 accumulation, either the coats were chemically cross-linked or binding was carried out at low pH (6.0), which stabilizes the coats enough to prevent disassembly. The dissociation rate constant was measured, after replacing the solution containing Hsc70-AF568 with uncoating buffer (pH 6.8) plus 2 mM ATP, by following the decrease of the Hsc70-AF568 signal from intact coats and calculated to be $0.027 \pm 0.001\ \text{s}^{-1}$ and $0.028 \pm 0.003\ \text{s}^{-1}$ for cross-linked coats and low pH stabilized coats, respectively. The corresponding mean residence time, about 40 s, is comparable to the accumulation time at the Hsc70 concentrations we have used. Thus, some Hsc70 exchange occurs during the course of the accumulation phase. This effect is probably negligible at the more than tenfold higher Hsc70 concentrations in cells. Note that some of the Hsc70-AF568 bound coats stabilized at low pH can transition to the disassembly phase upon shifting the pH to 6.8. Hsc70 dissociation is sufficiently

rapid, however, that with no free Hsc70 in the solution, many coats do not begin to disassemble before the level of bound Hsc70 has become too low to initiate uncoating.

Stepwise binding model for Hsc70-mediated uncoating. We describe Hsc70 binding to a clathrin coat as a stepwise process (Fig. 6a), with the microscopic rate constants estimated as described above. The absence of saturation in the observed Hsc70-binding fluorescence traces (Fig. 3a) suggests that uncoating begins when a critical number of Hsc70 molecules have bound. If we instead assume that all binding sites must be filled to initiate the uncoating reaction, the model predicts association times that extend far beyond those observed (similarly, a Michaelis-Menten-type model cannot reproduce the observed accumulation time distributions). Denoting the critical number of bound Hsc70 as N_t, the binding step states in the model of Fig. 6a can be described by a system of differential equations of the form

$$\frac{\partial S_0}{\partial t} = -Nk_1^+ S_0 + k_1^- S_1$$
$$\frac{\partial S_n}{\partial t} = -(nk_1^- + (N-n)k_1^+)S_n + (N-n+1)k_1^+ S_{n-1} + (n+1)k_1^- S_{n+1} \qquad (2)$$
$$\frac{\partial S_{N_t}}{\partial t} = -(N_t k_1^- + k_2^+)S_{N_t} + (N-N_t+1)k_1^+ S_{N_t-1}$$

under the initial conditions $S_0 = 1$, $S_{1...N_t} = 0$, i.e., with all coats free of bound Hsc70. The probability density function for the Hsc70 accumulation time is then given by the state $S_{N_t}(t)$.

To estimate the free model parameter N_t we minimized the χ^2 distance between the empirical cumulative distribution of accumulation times and the cumulative distribution function predicted by the model. Given an initial guess of N_t, the accumulation time distribution was computed by solving the equation system (2) using the ode45 solver in Matlab (The MathWorks, Inc.). The fit consistently yielded an unambiguous global minimum at $N_t = 18$ for the accumulation time distributions across all measured concentrations (Supplementary Fig. 10). At two concentrations (0.9 μM and 0.6 μM), the Kolmogorov-Smirnov test indicated that the model accurately describes the data with a 0.95 significance level (p-value > 0.03).

Estimation of the rate constant k_2^+. To separate the kinetics of the transition to coat disassembly from the kinetics of Hsc70 binding, we stabilized the coats at low pH while binding auxilin and Hsc70 and then shifted the pH to 6.8 to trigger the uncoating reaction of the auxilin/Hsc70 loaded coats (Figure 7). The conditions we used for the binding of uncoating reagents at low pH were similar to those used to prepare auxilin/Hsc70 bound coats for electron cryomicroscopy (Xing, Y. et al. *EMBO J* **29**, 655–65 (2010)). Under these conditions the coats remain intact, and we observed no decrease in their fluorescence intensity. To trigger the uncoating reaction, uncoating buffer (pH 6.8) containing auxilin and unlabeled Hsc70 and was flushed into the flow channel. It was necessary to maintain a supply of uncoating enzymes during the pH shift because the dissociation of Hsc70 from the coats was rapid enough that the uncoating reaction could not proceed in its absence (see above).

The waiting time distribution measured from the time of the pH shift to the start of disassembly can be described by a single exponential decay (Figure 7b), consistent with the presence of a single

rate-limiting step described by the rate constant k_2^+ (estimated to be $0.16 \pm 0.1\ \text{s}^{-1}$). This rate constant describes the "unlocking" associated with the removal of the first triskelion(s) from a coat loaded with N_t Hsc70 molecules.

Estimation of the rate constant k_3^+. The rate of the uncoating phase was estimated by fitting the proposed model, extended by an additional disassembly step, to the uncoating time distributions. As evident from the distribution of disassembly times (Fig. 6a, insets), this last step depends linearly on the Hsc70 concentration, which determines the probability that a critical number of the remaining vertices will be occupied at any time during the disassembly phase. A global fit over the measured concentrations yielded the first order rate constant $k_3^+ = 0.105\ \mu\text{M}^{-1}\text{s}^{-1}$.

The rate of the uncoating phase derived from our analysis of the single particle uncoating traces is an overestimate of the real rate because the disassembly phase is not always observed in its entirety in the single particle assay. Uncoating traces can be truncated when the clathrin that holds the coat onto the surface is removed from the coat; the coat, no longer bound to the substrate, diffuses away from its original location, resulting in an underestimate of the disassembly time for that trace.